

Study of the Λ/Σ^0 electroproduction in the low- Q^2 region at JLab

K. Okuyama^{1,*}, K. Itabashi¹, S. Nagao¹, S. N. Nakamura^{1,2}, K. N. Suzuki³, T. Gogami³, B. Pandey⁴, L. Tang^{4,5}, D. Abrams⁶, T. Akiyama¹, D. Androic⁷, K. Aniol⁸, C. Ayerbe Gayoso⁹, J. Bane¹⁰, S. Barcus⁹, J. Barrow¹⁰, V. Bellini¹¹, H. Bhatt¹², D. Bhetuwal¹², D. Biswas⁴, A. Camsonne⁵, J. Castellanos¹³, J-P. Chen⁵, J. Chen⁹, S. Covrig⁵, D. Chrisman^{14,15}, R. Cruz-Torres¹⁶, R. Das¹⁷, E. Fuchey¹⁸, K. Gnanvo⁶, F. Garibaldi^{11,19}, T. Gautam⁴, J. Gomez⁵, P. Gueye⁴, T. J. Hague²⁰, O. Hansen⁵, W. Henry⁵, F. Hauenstein²¹, D. W. Higinbotham⁵, C. E. Hyde²¹, M. Kaneta¹, C. Keppel⁵, T. Kutz¹⁷, N. Lashley-Colthirst⁴, S. Li^{22,23}, H. Liu²⁴, J. Mammei²⁵, P. Markowitz¹³, R. E. McClellan⁵, F. Meddi^{11,26}, D. Meekins⁵, R. Michaels⁵, M. Mihovilovic^{27,28,29}, A. Moyer³⁰, D. Nguyen^{16,31}, M. Nycz²⁰, V. Owen⁹, C. Palatchi⁶, S. Park¹⁷, T. Petkovic⁷, S. Premathilake⁶, P. E. Reimer³², J. Reinhold¹³, S. Riordan³², V. Rodriguez³³, C. Samanta³⁴, S. N. Santiesteban²², B. Sawatzky⁵, S. Širca^{27,28}, K. Slifer²², T. Su²⁰, Y. Tian³⁵, Y. Toyama¹, K. Uehara¹, G. M. Urciuoli¹¹, D. Votaw^{14,15}, J. Williamson³⁶, B. Wojtsekhowski⁵, S. A. Wood⁵, B. Yale²², Z. Ye³², J. Zhang⁶, and X. Zheng⁶

¹Department of Physics, Graduate School of Science, Tohoku University, Sendai, Miyagi 980-8578 Japan

²Department of Physics, Graduate School of Science, The University of Tokyo, Hongo, Tokyo 113-0033 Japan

³Department of Physics, Graduate School of Science, Kyoto University, Kyoto, Kyoto 606-8502 Japan

⁴Department of Physics, Hampton University, Hampton, Virginia 23668, USA

⁵Thomas Jefferson National Accelerator Facility, Newport News, Virginia 23606, USA

⁶Department of Physics, University of Virginia, Charlottesville, Virginia 22904, USA

⁷Department of Physics & Department of Applied Physics, University of Zagreb, HR-10000 Zagreb, Croatia

⁸Physics and Astronomy Department, California State University, Los Angeles, California 90032, USA

⁹Department of Physics, The College of William and Mary, Virginia 23185, USA

¹⁰Department of Physics, University of Tennessee, Knoxville, Tennessee 37996, USA

¹¹Istituto Nazionale di Fisica Nucleare, Sezione di Roma, 00185, Rome, Italy

¹²Department of Physics, Mississippi State University, Mississippi State, Mississippi 39762, USA

¹³Department of Physics, Florida International University, Miami, Florida 33199, USA

¹⁴Department of Physics and Astronomy, Michigan State University, East Lansing, Michigan 48824, USA

¹⁵National Superconducting Cyclotron Laboratory, Michigan State University, East Lansing, MI 48824, USA

¹⁶Department of Physics, Massachusetts Institute of Technology, Cambridge, Massachusetts 02139, USA

¹⁷Department of Physics, State University of New York, Stony Brook, New York 11794, USA

¹⁸Department of Physics, University of Connecticut, Storrs, Connecticut 06269, USA

¹⁹Istituto Superiore di Sanità, 00161, Rome, Italy

²⁰Department of Physics, Kent State University, Kent, Ohio 44242 USA

²¹Department of Physics, Old Dominion University, Norfolk, Virginia 23529, USA

*e-mail: kazuki@lambda.phys.tohoku.ac.jp

²²Department of Physics, University of New Hampshire, Durham, New Hampshire 03824, USA

²³Nuclear Science Division, Lawrence Berkeley National Laboratory, Berkeley, CA 94720, USA

²⁴Department of Physics, Columbia University, New York, New York 10027, USA

²⁵Department of Physics and Astronomy, University of Manitoba, Winnipeg, Manitoba R3T 2N2, Canada

²⁶Sapienza University of Rome, I-00185, Rome, Italy

²⁷Faculty of Mathematics and Physics, University of Ljubljana, 1000 Ljubljana, Slovenia

²⁸Jožef Stefan Institute, Ljubljana, Slovenia

²⁹Institut für Kernphysik, Johannes Gutenberg-Universität Mainz, DE-55128 Mainz, Germany

³⁰Department of Physics, Christopher Newport University, Newport News, Virginia 23606, USA

³¹University of Education, Hue University, Hue City, Vietnam

³²Physics Division, Argonne National Laboratory, Lemont, Illinois 60439, USA

³³División de Ciencias y Tecnología, Universidad Ana G. Méndez, Recinto de Cupey, San Juan 00926, Puerto Rico

³⁴Department of Physics & Astronomy, Virginia Military Institute, Lexington, Virginia 24450, USA

³⁵Department of Physics, Syracuse University, New York, New York 10016, USA

³⁶School of Physics & Astronomy, University of Glasgow, Glasgow, G12 8QQ, Scotland, UK

Abstract. We performed an experiment using tritium and hydrogen cryogenic gas targets at Thomas Jefferson National Accelerator Facility (JLab) in 2018 (E12-17-003)[1, 2]. In this article, we discuss the Λ/Σ^0 hyperon electroproduction from hydrogen target. Elementary Λ/Σ^0 hyperon production processes are important not only for an absolute mass scale calibration in our experiment, but also for the study of the electroproduction mechanisms themselves. In this article, we reported the results of the differential cross section for the $p(e, e' K^+) \Lambda/\Sigma^0$ reaction at $Q^2 \sim 0.5$ (GeV/c)².

1 Introduction

We have started and proceeded Λ hypernuclear experiments at JLab to understand the hyperon-nucleon interaction from the binding energy measurements of hypernuclei. Our experimental method enables us to investigate not only Λ hyperon but also Σ^0 hyperon production processes simultaneously as described later on. Λ/Σ^0 photoproduction $p(\gamma, K^+) \Lambda/\Sigma^0$ and electroproduction $p(e, e' K^+) \Lambda/\Sigma^0$ have been studied over several decades. In both reactions, protons are converted to hyperons. The only difference between them is that the photon involved in the reaction is real or virtual.

Experimentally, hyperon photoproduction has been studied very well and an abundance of data has been reported by many experimental groups[3–8]. Meanwhile, hyperon electroproduction can be associated with hyperon photoproduction and studied in a complementary manner under the same theoretical framework. The contribution from the virtual photon can be extracted by factorizing the triple differential cross section as follows[9]:

$$\frac{d^3\sigma}{d\omega d\Omega_{e'} d\Omega_K^{c.m.}} = \Gamma \frac{d\sigma_{\gamma^*}}{d\Omega_K^{c.m.}}, \quad (1)$$

where Γ is a so-called virtual photon flux. Through its definition, $d\sigma_{\gamma^*}/d\Omega_K^{c.m.}$ is regarded as a differential cross section for the kaon-hyperon production from virtual photons. Four-momentum of a virtual photon is denoted as $q^\mu := (\omega, \mathbf{q}) = (E_e - E_{e'}, \mathbf{P}_e - \mathbf{P}_{e'})$.

In the case of hyperon electroproduction, data can be taken at forward angles along the virtual photon direction, which are regions of interest for the photoproduction because it is missing. Besides that, $Q^2 := -q^2$ dependency appears in the electroproduction and this is also

interesting and promising. However, experimental data on electroproduction is less abundant than that on photoproduction. Thus, providing the results of the differential cross section for the hyperon electroproduction from experimental side is necessary.

2 Experiment

2.1 Missing mass method

We used 4.32-GeV electron beams provided by CEBAF (Continuous Electron Beam Accelerator Facility) at JLab and hydrogen gas as a fixed proton target. We measured momenta of the scattered final electrons ($\sim 2.10 \text{ GeV}/c$) and positively charged kaons ($\sim 1.82 \text{ GeV}/c$) associated with the neutral charged hyperon production in coincidence by using large magnetic spectrometers, HRS-L and HRS-R, respectively. Detailed descriptions of the experimental setup can be found in following papers[1, 10, 11]. Eventually, missing mass is calculated from the momentum-energy conservation for every coincidence event by

$$\text{Missing Mass} = \sqrt{E_{\text{miss}}^2 - \mathbf{P}_{\text{miss}}^2} = \sqrt{(E_e - E_{e'} + M_p - E_K)^2 - (\mathbf{P}_e - \mathbf{P}_{e'} - \mathbf{P}_K)^2}. \quad (2)$$

With proton target, peaks at masses of Λ and Σ^0 are observed in the spectrum as shown in figure 1. Backgrounds come from the $\text{Al}(e, e'K^+)X$ reaction because of the target cell made of Aluminum and the $p(e, e'\pi^+)X$ reaction because of the high rate of pions. Amount and distribution of these background source are estimated and indicated by a yellow line in figure 1 even though they are very small. Therefore, remaining events are considered to be truly the hyperon production events. The tail structure from each peak is considered as a radiative tail. Radiative tail is well-understood phenomenon in the electron scattering experiment because electrons easily emit radiations. In this case, it was mainly caused from the scattered electrons when they pass through the Aluminum target cell obliquely. In order to derive the differential cross sections, radiative tail also needs to be taken into account as a hyperon production events. Those estimations were performed by fitting the distribution in some ways, combined with adequate simulation. The fluctuations of the fitting results are included as systematic uncertainties.

2.2 Differential cross section derivation

Differential cross sections are deduced using a following formula,

$$\left(\frac{d\sigma_{\gamma^* p \rightarrow K^+ \Lambda(\Sigma^0)}}{d\Omega_{K^+}} \right)_{\text{HRS-R}} = \frac{1}{N_T} \cdot \frac{1}{N_{\gamma^*}} \cdot \frac{1}{\bar{\epsilon}} \cdot \sum_{i=1}^{N_{\Lambda(\Sigma^0)}} \frac{1}{\varepsilon_i^{\text{DAQ}} \cdot \varepsilon_i^{\text{Decay}} \cdot \Delta\Omega_{\text{HRS-R},i}}, \quad (3)$$

where, N_T is the number of proton targets per unit area, N_{γ^*} is the number of virtual photons contributing to the production, and $\bar{\epsilon}$ is the cut efficiency in the event selection. In particular, data acquisition efficiency $\varepsilon_i^{\text{DAQ}}$, K^+ 's survival ratio without any decay $\varepsilon_i^{\text{Decay}}$, and solid angle of HRS-R $\Delta\Omega_{\text{HRS-R},i}(p_K, Z)$ as a function of momentum and reaction point are applied every i -th event. Estimated quantities are summarized in table 1.

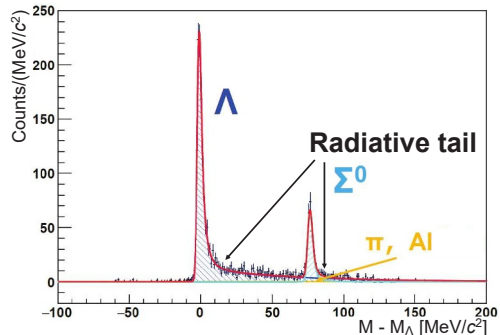


Figure 1. Missing mass spectrum obtained by the $p(e, e'K^+)X$ reaction. It was fitted to estimate number of hyperons including radiative tails (see text).

Figure 1 shows the missing mass spectrum obtained by the $p(e, e'K^+)X$ reaction. The x-axis represents the missing mass $M - M_\Lambda$ in MeV/c^2 , ranging from -100 to 200. The y-axis represents the count rate in MeV/c^2 , ranging from 0 to 250. The spectrum features two distinct peaks: a sharp red peak at $M - M_\Lambda \approx 0$ labeled Λ , and a broader blue peak at $M - M_\Lambda \approx 80$ labeled Σ^0 . A yellow line labeled π, Al represents the background. A black line labeled "Radiative tail" shows the tail of the Σ^0 peak. The plot is fitted to estimate the number of hyperons including radiative tails.

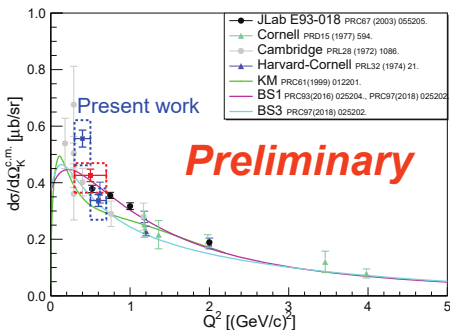
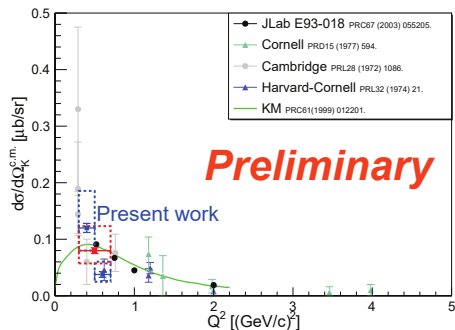
Differential cross sections are deduced using a following formula,

$$\left(\frac{d\sigma_{\gamma^* p \rightarrow K^+ \Lambda(\Sigma^0)}}{d\Omega_{K^+}} \right)_{\text{HRS-R}} = \frac{1}{N_T} \cdot \frac{1}{N_{\gamma^*}} \cdot \frac{1}{\bar{\epsilon}} \cdot \sum_{i=1}^{N_{\Lambda(\Sigma^0)}} \frac{1}{\varepsilon_i^{\text{DAQ}} \cdot \varepsilon_i^{\text{Decay}} \cdot \Delta\Omega_{\text{HRS-R},i}}, \quad (3)$$

where, N_T is the number of proton targets per unit area, N_{γ^*} is the number of virtual photons contributing to the production, and $\bar{\epsilon}$ is the cut efficiency in the event selection. In particular, data acquisition efficiency $\varepsilon_i^{\text{DAQ}}$, K^+ 's survival ratio without any decay $\varepsilon_i^{\text{Decay}}$, and solid angle of HRS-R $\Delta\Omega_{\text{HRS-R},i}(p_K, Z)$ as a function of momentum and reaction point are applied every i -th event. Estimated quantities are summarized in table 1.

Table 1. Estimated quantities with statistical errors for deriving the differential cross sections

	Λ	Σ^0
N_T	$0.0375 \pm 0.0013 [\text{b}^{-1}]$	
$N_{\gamma^*}/10^{13}$	3.53 ± 0.01	4.95 ± 0.01
$\bar{\varepsilon}$	$45.4 \pm 1.2 [\%]$	$44.3 \pm 1.2 [\%]$
$N_{\text{Hyperon}}/10^3$	1.36 ± 0.04	0.37 ± 0.02
$\varepsilon^{\text{Decay}}$	$\sim 14 [\%]$	$\sim 14 [\%]$
ε^{DAQ}	$\sim 96 [\%]$	$\sim 96 [\%]$
$\Delta\Omega_{\text{HRS-R}}^{\text{Lab}}$	$\sim 5.5 [\text{msr}]$	

**Figure 2.** The Q^2 dependency of the differential cross sections for the Λ hyperon electro-production (see text).**Figure 3.** The Q^2 dependency of the differential cross sections for the Σ^0 hyperon electro-production (see text).

3 Results

Using the dataset of our experiment ($W \sim 2.14 \text{ GeV}$, $Q^2 \sim 0.5 \text{ (GeV/c)}^2$, $\theta_{\gamma K}^{\text{c.m.}} \sim 8 \text{ deg}$), we deduced the differential cross sections. In next subsections, we discuss these results comparing with other experimental data and theoretical calculations by showing the Q^2 dependency and angle dependency.

3.1 Q^2 dependency

The obtained results are shown with Q^2 dependency of the differential cross section in figure 2 and figure 3. Red points are the results using all data and blue points are the results with data divided into 2 sets based on Q^2 to see its dependency. Our results show the statistical error by the solid lines and the dotted boxes include systematic error. The other experimental results show only the statistical error[12–15]. Theoretical results are shown by curved lines[16–18]. As Q^2 decreases, our results tend to increase, which are similar to the other results, but with a higher slope.

3.2 Angle dependency

The obtained results are shown with angle dependency of the differential cross section in figure 4 and figure 5. Experimental data and theoretical calculations for the photoproductions are also shown without corrections[3–8, 16, 19, 20]. We deduced the differential cross section in low- Q^2 regions at forward angles which is missing data in the photoproductions. Our results tend to decrease as they approach to the forward angles in both reactions, but almost flat for Λ within statistical errors.

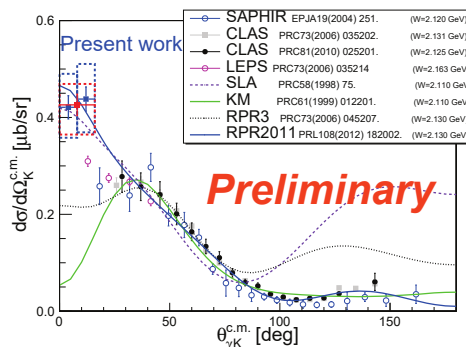


Figure 4. The $\theta_{\gamma K}^{\text{c.m.}}$ dependency of the differential cross sections for the Λ hyperon production. Our data is at $Q^2 \sim 0.5$ (GeV/c) 2 , the others are at $Q^2 = 0$ (see text).

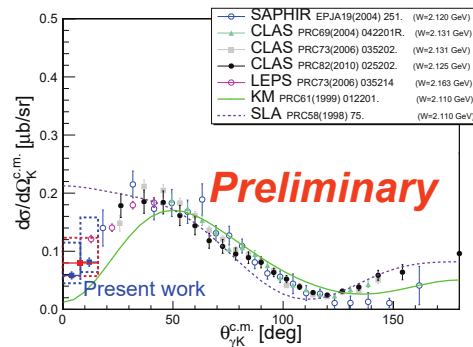


Figure 5. The $\theta_{\gamma K}^{\text{c.m.}}$ dependency of the differential cross sections for the Σ^0 hyperon production. Our data is at $Q^2 \sim 0.5$ (GeV/c) 2 , the others are at $Q^2 = 0$ (see text).

4 Summary

We performed E12-17-003 experiment at JLab in 2018. This article described the results of the differential cross sections for the Λ/Σ^0 hyperon electroproduction at forward angles in low- Q^2 region. This is a region of interest where there was no data in the photoproduction so far. This work helps understanding hyperon photoproduction and electroproduction in the same theoretical framework.

5 Acknowledgement

We thank the JLab staff of the Division of Physics, Division of Accelerator, and the Division of Engineering for providing support for conducting the experiment. This work was supported by U.S. Department of Energy (DOE) grant DE-AC05-06OR23177 under which Jefferson Science Associates, LLC, operates the Thomas Jefferson National Accelerator Facility. The work of the Argonne National Laboratory group member is supported by DOE grant DE-AC02-06CH11357. The Kent State University contribution is supported under grant no. PHY-1714809 from the U.S. National Science Foundation. The hypernuclear program at JLab is supported by U.S. DOE grant DE-FG02-97ER41047. This work was partially supported by the Grant-in-Aid for Scientific Research on Innovative Areas “Toward new frontiers Encounter and synergy of state-of-the-art astronomical detectors and exotic quantum beams.” This work was supported by JSPS KAKENHI grants nos. 18H05459, 18H05457, 18H01219, 17H01121, 19J22055, and 18H01220. This work was also supported by the Graduate Program on Physics for the Universe, Tohoku University (GP-PU), and SPIRITS 2020 of Kyoto University.

References

- [1] K.N. Suzuki, T. Gogami et al., *Prog. Theor. Exp. Phys.* **2022**, 013D01 (2022)
- [2] B. Pandey, L. Tang et al., *Phys. Rev. C* **105**, L051001 (2022)
- [3] K.H. Glander, J. Barth et al., *Eur. Phys. J. A* **19**, 251 (2004)
- [4] R. Bradford, R.A. Schumacher et al., *Phys. Rev. C* **73**, 035202 (2006)
- [5] M.E. McCracken, M. Bellis et al., *Phys. Rev. C* **81**, 025201 (2010)
- [6] M. Sumihama, J.K. Ahn et al., *Phys. Rev. C* **73**, 035214 (2006)

- [7] J.W.C. McNabb, R.A. Schumacher et al., *Phys. Rev. C* **69**, 042201 (2004)
- [8] B. Dey, C.A. Meyer et al., *Phys. Rev. C* **82**, 025202 (2010)
- [9] E. Amaldi, S. Fubini et al., *Pion Electroproduction. Electroproduction at Low- Energy and Hadron Form-Factors*, Vol. 83 (Springer Tracts in Modern Physics, 1979)
- [10] J. Alcorn, B. Anderson et al., *Nucl. Instrum. Methods, Phys. Res. Sect. A* **522**, 294 (2004)
- [11] S. Santiesteban, S. Alsalmi et al., *Nucl. Instrum. Methods, Phys. Res. Sect. A* **940**, 351 (2019)
- [12] R.M. Mohring, D. Abbott et al., *Phys. Rev. C* **67**, 055205 (2003)
- [13] C.J. Bebek, C.N. Brown et al., *Phys. Rev. D* **15**, 594 (1977)
- [14] C.N. Brown, C.R. Canizares et al., *Phys. Rev. Lett.* **28**, 1086 (1972)
- [15] C.J. Bebek, C.N. Brown et al., *Phys. Rev. Lett.* **32**, 21 (1974)
- [16] T. Mart, C. Bennhold, *Phys. Rev. C* **61**, 012201 (1999)
- [17] D. Skoupil, P. Bydžovský, *Phys. Rev. C* **93**, 025204 (2016)
- [18] D. Skoupil, P. Bydžovský, *Phys. Rev. C* **97**, 025202 (2018)
- [19] T. Corthals, J. Ryckebusch et al., *Phys. Rev. C* **73**, 045207 (2006)
- [20] L. De Cruz, T. Vrancx et al., *Phys. Rev. Lett.* **108**, 182002 (2012)